Scientific Research Publishing

Open Journal of Civil Engineering, 2020, 10, 83-92
https://www.scirp.org/journal/ojce
ISSN Online: 2164-3172
ISSN Print: 2164-3164

Theoretical Analysis of Simulating the Locked-In Stress in Rock Pore by Thermal Expansion of Hard Rubber

Lu Dong, Hansheng Geng*, Hongfa Xu, Yinhao Yang

State Key Laboratory of Disaster Prevention and Mitigation of Explosion and Impact, National Defense Engineering College, Army Engineering University of PLA, Nanjing, China
Email: *genghansheng@163.com

How to cite this paper: Dong, L., Geng, H.S., Xu, H.F. and Yang, Y.H. (2020) Theoretical Analysis of Simulating the Locked-In Stress in Rock Pore by Thermal Expansion of Hard Rubber. *Open Journal of Civil Engineering*, **10**, 83-92.
https://doi.org/10.4236/ojce.2020.102008

Received: March 5, 2020
Accepted: March 27, 2020
Published: March 30, 2020

Abstract

Rocks are composed of mineral particles and micropores between mineral which has a great influence on the mechanical properties of rocks. In this paper, based on the theory of locked-in stress developed by academician Chen Zongji, the locked-in stress problem in underground rock is simulated by the thermal expansion of hard rubber particles. The pore inclusion in rock is assumed to be uniformly distributed spherical cavities. Using the thermal stress theory, the stress of rock with a spherical pore inclusion is equivalent to the thermal stress generated by the spherical hard rubber inclusion. The elastic theory formula of the temperature increment and the equivalent pore pressure of the spherical hard rubber inclusion is derived. The numerical simulation of the rock mass model with a spherical hard rubber inclusion is carried out and compared to the theoretical calculation results; the results show that they are consistent. The method proposed by this paper for simulating stress distribution in rock by thermal stress is reasonable and feasible; it has a positive meaning for further study of mechanic phenomenon of rock with micropore inclusion.

Keywords

Rock Pore, Locked-In Stress, Similar Simulation, Rubber Particles, Thermal Expansion

1. Introduction

Rocks with randomly distributed inclusions can be considered as natural composite material. The main component of rock can be regarded as the matrix of composite material; cracks, heterogeneous particles, and pores in the rock can be

regarded as inclusions in composite material [1]. Normally, there exists fluid in micropore (liquid or gas), which affects the rock mechanical properties significantly. In the past, rocks containing micropores are equivalent to continuum macroscopically, but many phenomena can't be described by this solution. The elastic properties of composite materials are important issues and many theoretical results have been achieved so far. For engineering, rock is generally in elastic deformation stage before yielding. In this article, the micromechanics theory was used to study the elastic properties of rock containing inclusions. So far, many achievements have been made in the study of locked-in stresses in metals, but there is little research on locked-in stresses in rocks. Therefore, this article will further study the situation of inclusion with locked-in stresses.

In 1979, Mr. Chen-Zongji proposed locked-in stress hypothesis; he believes that creep and locked-in stress are two fundamental factors of rock characters [2] [3] [4]. The hypothesis is that: the hydrostatic pressure is small in the upper crust the projected involved. In this site, the grain boundary cracked because of the non-compatible strain effect, and the pore formed because of the splitting and non-uniform plastic flow of some particles. A part of concentrated stress releases in this way, and the other preserves in the form of locked-in stress. Over the years, this hypothesis has not been considerably developed. Academician Qian-Qihu proposed incompatible deformation problem of micropores, which studied the effect of the density and length of microcrack to self-balancing "locked-in stress" and rock damage [5] [6]. Wang-Mingyang and Li Jie researched the mechanism of rockburst from the perspective of the release of locked-in stress [7]. Yue-Zhongqi proposed and tried to demonstrate that the pressure and volume expansion energy of the fluid inclusions is one particular form of presence and action of locked-in stress and strain energy. He further proposed, analyzed and demonstrated that the microfluid inclusion locked in rock may be in compressed state, which can have a strong high pressure and cause local abnormally high stress field in the rock internal. Excavation of rock can lead to re-flow, movement and phase change over time of many microfluid inclusions with high pressure locked in rock [8] [9].

The locked-in stress is difficult to remain in rock in long term. Generally, after sampled from site, locked-in stress in the sample will slowly disappear due to the release of ground stress and environmental fluid (oil, water, gas) pressure. It is a problem long term concerned by scholars to simulate the locked-in stress of pores of the rock in underground environment.

This paper considers to simulating the locked-in stress exist in rocks in the underground environment by thermal expansion stress of hard rubber particles. Using the basic principles of the equivalent stress field, rocks containing pressure air inclusions are equivalent to rocks contains hard rubber inclusions. Expansion stress generated in the rocks because of the different linear expansion coefficient of rocks and hard rubber. The internal stress generated by the hard rubber inclusions in different temperature conditions is derived and compared

to numerical simulation results. The results of this paper are instructive about the construction of similar material of rocks contain locked-in stress.

2. A Simplified Model of a Spherical Pore Inclusion

For simplicity, the closed pores in rocks are assumed to be spherical and homogeneously distributed. Therefore, the rock can be divided into several units that arranged uniformly periodic and each unit is composed of rock matrix and spherical pore inclusion in it, as shown in Figure 1. According to the research needs, We can take 1/2 unit cell, 1/4 unit cell or 1/8 unit cell as a representative of the microscopic geometry unit [10], without considering gravity.

Under a certain depth, pressure is generated in closed pores inside the rock because of the initial *in-situ* stress. However, in the actual study, it is difficult to know this pressure, and it is difficult to obtain a specific pore pressure in the rock in the laboratory. This paper considers using equivalent stress field method, using high-strength cement to simulate rock matrix, and doping spherical hard rubber particle in it. Since the thermal expansion coefficient of hard rubber cement is much greater than rock, the gas pressure of the pore inclusion in the rock can be replaced by thermal stress generated by the temperature rise in the cement.

3. Thermal Stress Analysis of Hard Rubber Particle Inclusion

This section obtains the relationship between thermal stress of hard rubber inclusion and pressure of the spherical holes by analyzing the stress of thick-walled ball. Assuming that the radius of the pore is small enough with respect to the unit cell, it can be simplified as thick-walled sphere model with internal pressure, as shown in Figure 2.

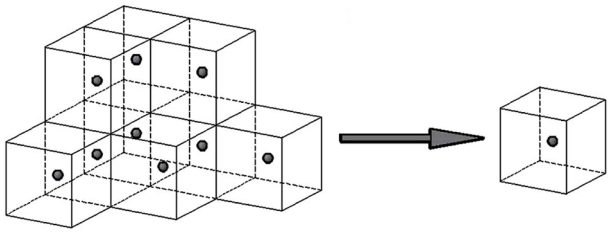

Figure 1. The simplified model of rock contains a spherical pore inclusion.

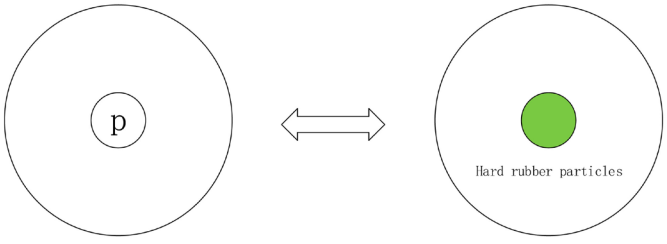

Figure 2. Equivalent model of thick-walled ball with internal pressure.

3.1. Analysis of Thick-Walled Ball

Assuming that the outer diameter of the thick-walled ball is b, and the inner diameter is a, the internal pressure is p_1, and external pressure is zero. Stress, strain and displacement at any point can be obtained according to reference [11]:

$$\sigma_r = \frac{a^3\left(r^3 - b^3\right)}{r^3\left(b^3 - a^3\right)} p_1 \tag{1}$$

$$\sigma_\theta = \frac{a^3\left(2r^3 + b^3\right)}{2r^3\left(b^3 - a^3\right)} p_1 \tag{2}$$

$$u = \frac{1}{E\left(b^3 - a^3\right)}\left[\left(1-2\mu\right)a^3 p_1 r + \frac{1+\mu}{2r^2} a^3 b^3 p_1\right] \tag{3}$$

where σ_r and σ_θ are the radial and tangential normal stress of the thick-walled ball, and u is the displacement component, E and μ is the elastic modulus and Poisson's ratio of matrix.

The inner wall displacement components of thick-walled ball are:

$$u_a = \frac{\left(1-2\mu\right)a^4 p_1 + \frac{1}{2}\left(1+\mu\right)ab^3 p_1}{E\left(-a^3 + b^3\right)} \tag{4}$$

where u_a is the inner wall displacement component of thick-walled ball.

For a is small enough, Equation (4) can be simplified as:

$$u_a = \frac{1+\mu}{2E} a p_1 \tag{5}$$

3.2. Analysis of Spherical Rubber Particle Inclusion

Replace the cavity in the thick-walled ball in 3.1 with hard rubber particles of the same geometry. Make the temperature rise ΔT, and remove the outside matrix, the change in volume caused by temperature changes of the hard rubber ball is:

$$\Delta V_1 = s \times \Delta T \times V_0 \tag{6}$$

where s and ΔV_1 are the volume expansion coefficient and volume increment of hard rubber when there is no external constraint.

Because the volume expansion coefficient of rock is far less than hard rubber, the volume expansion of rock matrix is ignored. Put the spherical hard rubber particle which has already expanded back into the pore, then it will be subjected to the external stress p_2 applied by the matrix, and volume change of the inclusion will be:

$$\Delta V_2 = -p_2 / K_1 \times \left(V_0 + \Delta V_1\right) \tag{7}$$

where K_1 indicates the bulk modulus of hard rubber, ΔV_2 is the volume increment of spherical hard rubber particle due to external constraint caused by the surrounding matrix.

The total volume increment of spherical particles of hard rubber is $\Delta V_m = \Delta V_1 + \Delta V_2$, namely:

$$\Delta V_m = \left(s \times \Delta T - p_2/K_1 - p_2 \times s \times \Delta t/K_1\right) \times V_0 \tag{8}$$

where $V_0 = \frac{4}{3}\pi a^3$ is the initial volume of spherical hard rubber particle and ΔV_m is the total volume increment.

Supposed the particle radius changes u totally after deformation, therefore:

$$\Delta V_m = \frac{4}{3}\pi(u+a)^3 - \frac{4}{3}\pi a^3 = \frac{4}{3}\pi a^3\left(s \times \Delta T - p_2/K_1 - p_2 \times s \times \Delta T/K_1\right) \tag{9}$$

Substitute Equation (5) into Equation (9), it can be obtained:

$$\frac{4}{3}\pi\left(\frac{1+\mu}{2E}ap_1 + a\right)^3 - \frac{4}{3}\pi a^3 = \frac{4}{3}\pi a^3\left(s \times \Delta T - p_2/K_1 - p_2 \times s \times \Delta T/K_1\right) \tag{10}$$

Due to the balance stress, $p_1 = p_2$, it can be obtained:

$$\frac{4}{3}\pi\left(\frac{1+\mu}{2E}ap_1 + a\right)^3 - \frac{4}{3}\pi a^3 = \frac{4}{3}\pi a^3\left(s \times \Delta T - p_1/K_1 - p_1 \times s \times \Delta T/K_1\right) \tag{11}$$

Simplify the Equation (11) to:

$$\left(\frac{1+\mu}{2E}p_1 + 1\right)^3 - 1 = \left(s \times \Delta T - p_1/K_1 - p_1 \times s \times \Delta T/K_1\right) \tag{12}$$

Expand Equation (12) to:

$$\left(\frac{1+\mu}{2E}p_1\right)^3 + 3\left(\frac{1+\mu}{2E}p_1\right)^2 + 3\left(\frac{1+\mu}{2E}p_1\right) = s\Delta T - \frac{p_1}{K_1} - \frac{p_1 s\Delta T}{K_1} \tag{13}$$

The order of magnitude of pore gas pressure p_1 is 10^6; the order of magnitude of rock elastic modulus E is 10^{-4}; the order of magnitude of volume expansion coefficient of hard rubber is 10^6; the order of magnitude of ΔT is 10^2; the order of magnitude of hard rubber's volume modulus is 10^7 - 10^8, therefore it is concluded that:

$$\left(\frac{1+\mu}{2E}p_1\right)^3 + 3\left(\frac{1+\mu}{2E}p_1\right)^2 + 3\left(\frac{1+\mu}{2E}p_1\right) \approx 3\left(\frac{1+\mu}{2E}p_1\right)$$

$$s\Delta T - \frac{p_1}{K_1} - \frac{p_1 s\Delta T}{K_1} \approx s\Delta T - \frac{p_1}{K_1}$$

Equation (13) can be simplified as:

$$p_1 = \frac{s}{\frac{3(1+\mu)}{2E} + \frac{1}{K_1}}\Delta T \tag{14}$$

Equation (14) expresses the pressure p_1 to the matrix generated by the model's temperature rise of ΔT. As shown in **Figure 3**, the temperature pressure curve of Equations (12) and (14) is almost identical in the range of 0 - 100, so Equation (12) can be replaced by Equation (14).

Stress distribution generated by the thermal expansion of spherical hard rubber particles in the thick-walled ball is obtained by combining Equations (1)-(3)

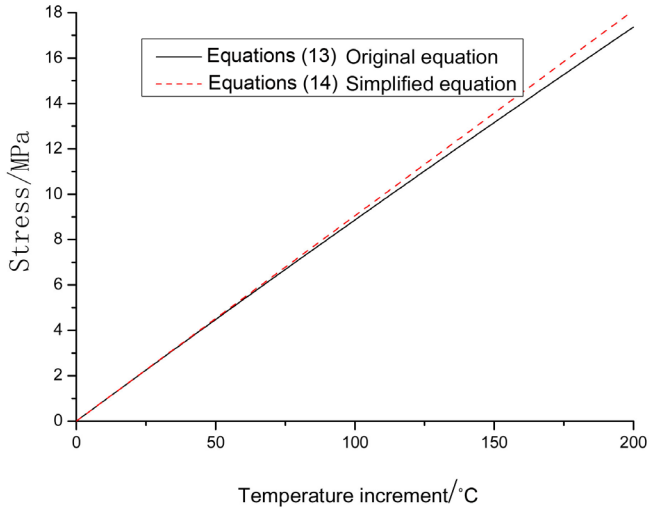

Figure 3. Comparison of theoretical results of temperature pressure curve of Formulas (12) and (14).

and (14).

$$\sigma_r = \frac{a^3\left(r^3 - b^3\right)s\Delta T}{r^3\left(b^3 - a^3\right)\left(\frac{3(1+\mu)}{2E} + \frac{1}{K_1}\right)} \tag{15}$$

$$\sigma_\theta = \frac{a^3\left(b^3 + 2r^3\right)s\Delta T}{2r^3\left(b^3 - a^3\right)\left(\frac{3(1+\mu)}{2E} + \frac{1}{K_1}\right)} \tag{16}$$

$$u = \frac{2r^3(1-2\mu)a^3 s\Delta T r + (1+\mu)a^3 b^3 s\Delta T}{2Er^3\left(b^3 - a^3\right)\left(\frac{3(1+\mu)}{2E} + \frac{1}{K_1}\right)} \tag{17}$$

4. Relationship between Average *In-Situ* Stress and Pore Pressure of Rocks

Without taking the tectonic stress into account, *in-situ* stress of rock satisfies:

$$\sigma_v = \rho g h \tag{18}$$

$$\sigma_H = \sigma_x = \sigma_y = \frac{\mu_0}{1-\mu_0}\rho g h \tag{19}$$

where ρ is the density of rock ($\rho = 2.7\ \mathrm{g \cdot cm^{-3}}$ for typical granodiorite on the earth's crust); g and h are the acceleration of gravity and depth; μ_0 is the rock Poisson ratio; σ_v and σ_H are the vertical crustal stress and the transverse stress.

σ_v, σ_x, σ_y are the first, second, and third principle stress.

The average *in-situ* stress of the rock will be:

$$\sigma_m = \frac{\sigma_v + \sigma_x + \sigma_y}{3} = \frac{1+\mu_0}{3(1-\mu_0)}\rho g h \tag{20}$$

According to reference [12], under the average *in-situ* stress σ_m, the pore pressure will be:

$$p_m = B\sigma_m + p_0 \tag{21}$$

Combine Equation (20) and (21):

$$p_m = \frac{1+\mu_0}{3(1-\mu_0)} B\rho gh + p_0 \tag{22}$$

where p_0 indicates standard atmospheric pressure, $p_0 = 1\times10^5$ Pa; B indicates the Skempton pore pressure coefficient, and the value of B is based on the reference [13]. In this paper, $B = 0.3$.

5. Numerical Simulation and Verification

This section verifies the theory of the previous paper by numerical simulation carried out by ANSYS-Mechanical. To establish a numerical model, the model length and width are 1cm, the radius of the spherical pore is 1mm, because of the pressure and gravity is not in an order of magnitude, so gravity does not take into account. After the rock sample removing from underground, the crustal stress disappears and the specimen is affected by pore pressure only. Set the Poisson's ratio μ of rock to be 0.3, the elastic modulus E to be 8×10^9; volume expansion coefficient of hard rubber to be $s = 2.53\times10^{-4}$; Poisson's ratio of hard rubber to be $\mu = 0.47$; and elastic modulus to be $E_1 = 7.8\times10^7$. Applying normal constraint on the three plane $x = 0$, $y = 0$, $z = 0$. The numerical model is shown in Figure 4.

5.1. Comparison of Theoretical and Numerical Simulation Results of One Point

Set the initial temperature of the model 0˚C, Temperature load of 10˚C, 20˚C, 30˚C, 40˚C, 50˚C, 60˚C, 70˚C, 80˚C, 90˚C is then applied as node load to the model respectively. Take the point of the 45 degree angle and radius 3 mm on the XY surface. Contrast and analyze the theoretical and numerical simulation results of this point, as shown in Figure 5.

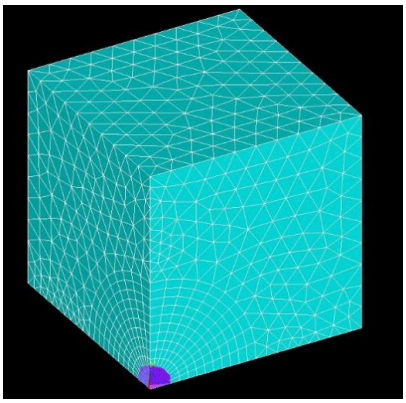

Figure 4. Numerical model of spherical rubber inclusion.

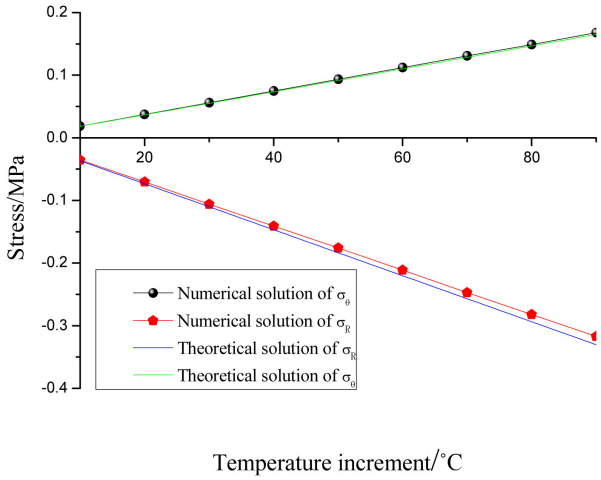

Figure 5. Comparison of the analytic solution and numerical analysis of stress of one point.

5.2. Compare Stress Simulation and Theoretical Solution at Selected Points at a Fixed Temperature

Assuming that the rock samples are taken from the depth of 1000 m. According to Equation (22) that the pore pressure at this site is 8.29 MPa, and equal to the thermal stress generated by the spherical hard rubber particle when the temperature rises 83.6˚C.

So the model is applied to a temperature load of 83.6˚C. **Figure 6** is the maximum principal stress cloud of this model.

Compare the theoretical analysis and numerical analysis results of stress at points from the Z-axis of the matrix geometry model and points at $r = 3$ mm in the XY plane, as shown in **Figure 7**.

As can be seen from **Figure 7**, on the Z-axis and XY plane, analytical and numerical analysis results of stress distribution agree well with each other.

6. Conclusions

In this paper, the pore inclusion in the rock is spherical, and pore pressure generates due to the effect of *in-situ* stress. Based on the theoretical derivation, combined with the actual situation, the stress of spherical pore inclusion is equivalent to the thermal stress generated by the spherical rubber inclusion according to the equivalent principle of the stress field. Through theoretical analysis and numerical simulation, the following results are obtained:

1) Theoretical formula of thermal stress equivalent pore inclusion pressure;

2) Empirical formula of the relationship between the depth of the rock and the pore pressure;

3) Theoretical analysis and numerical results are compared. Without taking into account the gravity effect, the two results agree well.

Combining the theoretical results of this paper with numerical simulation and experiment, the theoretical results of this paper are combined with numerical

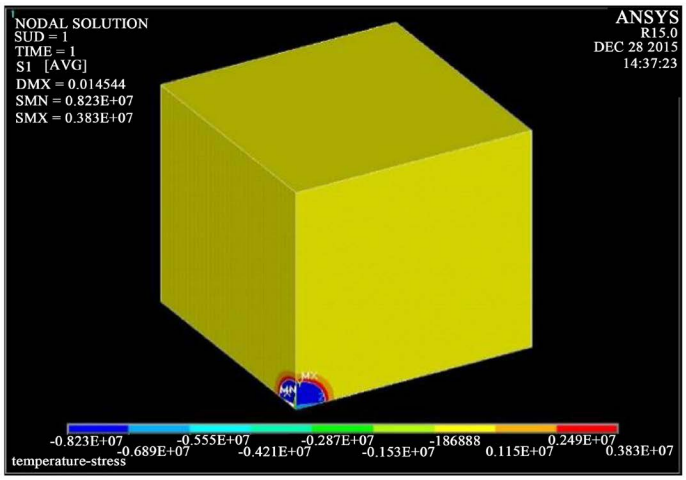

Figure 6. The maximum principal stress cloud.

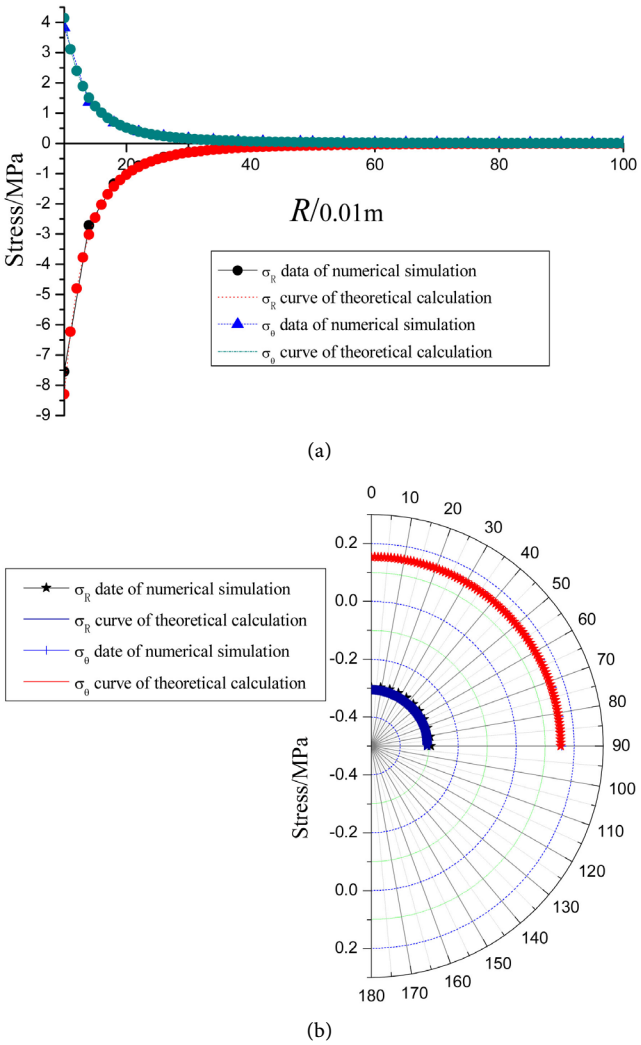

Figure 7. Comparison of the analytic solution and numerical analysis (vertical section). (a) Comparison of stress distribution in the Z-axis; (b) Comparison of stress distribution in the XY plane and at r = 30.

simulation and experiment. The stress distribution of rock with other shapes and pore inclusions can be further studied, which has a positive significance to the study of rock mechanics.

Acknowledgements

The authors gratefully acknowledge the financial supports to this work from Natural Science Found of Jiangsu Province (No. BK20190572).

Conflicts of Interest

The authors declare no conflicts of interest regarding the publication of this paper.

References

[1] Malik, A.S., Boyko, O., Atkar and Chen, Y. (2009) Rock Physics. Press of University of Science and Technology of China, Hefei.

[2] Kie, T.T. (1979) Vice-President Address Note. *Proceedings of Congress on Rock Mechanics of International Society for Rock Mechanics*, Montreux, Vol. 3, S253-S254.

[3] Tan, T.K. and Kang, W.F. (1980) Locked in Stresses, Creep and Dilatancy of Rocks, and Constitutive Equations. *Rock Mechanics*, **13**, 5-22. https://doi.org/10.1007/BF01257895

[4] Chen, Z.J., Kang, W.F. and Huang, J.F. (1991) On the Locked in Stress, Creep and Dilatation of Rocks, and the Constitutive Equations. *Chinese Journal of Rock Mechanic and Engineering*, No. 4, 299-312.

[5] Huang, S.J. and Hou, Z.J. (2001) Spatio-Temporal Variation of Subsurface Porosity and Permeability and Its Influential Factors. *Acta Sedimentologica Sinica*, **19**, 224-232.

[6] Qian, Q.H. and Zhou, X.P. (2013) Effects of Incompatible Deformation on Failure Mode and Stress Field of Surrounding Rock Mass. *Chinese Journal of Rock Mechanic and Engineering*, **32**, 649-656.

[7] Wang, M.Y., Li, J. and Li, K.R. (2015) A Nonlinear Mechanical Energy Theory in Deep Rock Mass Engineering and Its Application. *Chinese Journal of Rock Mechanic and Engineering*, No. 4, 659-667.

[8] Yue, Z.Q. (2014) Gas Inclusions and Their Expansion Power as Foundation of Rock "Locked-In" Stress Hypothesis. *Journal of Engineering Geology*, No. 4, 739-756.

[9] Yue, Z.Q. (2015) Expansion Power of Compressed Micro Fluid Inclusions as the Cause of Rockburst. *Mechanics in Engineering*, No. 3, 287-294.

[10] Suquet, P.M. (1987) Elements of Homogenization for Inelastic Solid Mechanics. In: Sanchez-Palencia, E. and Zaoui, A., Eds., *Homogenization Techniques for Composite Media*, Springer, Berlin, 193-279.

[11] Xu, B.Y. (1995) Application of Elastic and Plastic Mechanics. Tsinghua University Press, Beijing.

[12] Biot, M.A. (1941) General Theory of Three-Dimensional Consolidation. *Journal of Applied Physics*, **12**, 155-164. https://doi.org/10.1063/1.1712886

[13] Kopf, A., Paterson, M.S. and Wong, T.F. (2006) Experimental Rock Deformation—The Brittle Field, 2005. *Surveys in Geophysics*, **27**, 487-488. https://doi.org/10.1007/s10712-006-9004-5